JOURNAL OF NEUROTRAUMA 35:739–749 (March 1, 2018)

DOI: 10.1089/neu.2016.4944

Common Patterns of Regional Brain Injury Detectable by Diffusion Tensor Imaging in Otherwise Normal-Appearing White Matter in Patients with Early Moderate to Severe Traumatic Brain Injury

Kristine H. O'Phelan,[1] Chad K. Otoshi,[2] Thomas Ernst,[2,3] and Linda Chang[2,3]

Abstract

Traumatic brain injury (TBI) alters the lives of millions of people every year. Although mortality rates have improved, attributed to better pre-hospital care and reduction of secondary injury in the critical care setting, improvements in functional outcomes post-TBI have been difficult to achieve. Diffusion-tensor imaging (DTI) allows detailed measurement of microstructural damage in regional brain tissue post-TBI, thus improving our understanding of the extent and severity of TBI. Twenty subjects were recruited from a neurological intensive care unit and compared to 18 healthy control subjects. Magnetic resonance imaging (MRI) scanning was performed on a 3.0-Tesla Siemens TIM Trio Scanner (Siemens Medical Solutions, Erlangen, Germany) including T1- and T2-weighted sequences and DTI. Images were processed using DTIStudio software. SAS (SAS Institute Inc., Cary, NC) was used for statistical analysis of group differences in 14 brain regions (25 regions of interests [ROIs]). Seventeen TBI subjects completed scanning. TBI and control subjects did not differ in age or sex. All TBI subjects had visible lesions on structural MRI. TBI subjects had seven brain regions (nine ROIs) that showed significant group differences on DTI metrics (fractional anisotropy, radial diffusion, or mean diffusion) compared to noninjured subjects, including the corpus callosum (genu and splenium), superior longitudinal fasciculus, internal capsule, right retrolenticular internal capsule, posterior corona radiata, and thalamus. However, 16 ROIs showed relatively normal DTI measures. Quantitative DTI demonstrates multiple areas of microstructual injury in specific normal-appearing white matter brain regions. DTI may be useful for assessing the extent of brain injury in patients with early moderate to severe TBI.

Keywords: brain imaging; diffusion tensor imaging; head injury; MRI; traumatic brain injury

Introduction

Traumatic brain injury (TBI) continues to be an important cause of morbidity and mortality across people of all ages in all parts of the world. In the United States and Europe, incidence ranges from 180 to 500 per 100,000 persons per year.[1] TBI has gained public visibility in recent years because of increasing awareness of both clinically significant sports injuries as well as injured veterans who are returning with this diagnosis after their combat in the Middle East. In addition, substance use such as alcohol and methamphetamine use disorders are also major risk factors for motor vehicle accidents that can lead to TBI.

Our understanding of the multitude of variables influencing patient outcomes post-TBI is still evolving. Clinical therapies used to mitigate the effects of secondary injuries attributed to hypoxia, hypotension, hyperthermia, and seizures have become the mainstay of clinical care of acute TBI, but there has been little progress made to address the primary injury caused by TBI. Further, heterogeneity exists in regional brain metabolism post-TBI[2,3] which likely mirrors the diffuse, but variable, alterations in white matter integrity. Advancements in imaging technologies allow clinicians to identify structural injury in brain regions beyond those visible on conventional imaging, which may lead to many post-traumatic sequelae and has implications for acute and chronic care. One such imaging technique, diffusion tensor imaging (DTI), uses magnetic resonance (MR) imaging (MRI) to measure the direction of movement of water molecules in multiple planes and indirectly provide information about the microstructural integrity of the white matter

[1]Department of Neurology, Miller School of Medicine, University of Miami, Miami, Florida.
[2]Department of Medicine, Neuroscience and MRI Research Program, John A. Burns School of Medicine, University of Hawaii at Manoa, Honolulu, Hawaii.
[3]Department of Diagnostic Radiology and Nuclear Medicine, University of Maryland School of Medicine, Baltimore, Maryland.

tracts. These white matter connections are critical for cognitive and motor function during and after recovery from TBI. Several review articles described the utility of DTI in examining microstructural abnormalities in patients with TBI of varying severity.[4–6] These studies have shown significant abnormalities in white matter integrity post-TBI and correlation with functional outcome at chronic time points.[7] Additionally, a recent multi-center study demonstrated a significant correlation between quantitative regional DTI studies performed within the first 45 days post-injury and functional recovery at 1 year.[8]

The aim of this study is to assess quantitatively the disturbances of microstructural tissue integrity in brain regions involving major white matter tracts and subcortical structures in patients who sustained an acute TBI. Our study extends past work by using quantitative multi-regional measurements and describing common patterns of regional brain injury very early in the clinical course and in areas that appear normal on standard MRI. Additionally, because brain function depends on neural interconnectivity, a network approach has been used to examine DTI data from TBI patients.[9] Although we will not be evaluating the neural networks involved, identification of commonly affected brain regions with DTI may improve our understanding of functional connectivity failure observed post-TBI. Understanding which specific DTI metric, such as fractional anisotropy (FA), axial diffusivity (AD) or radial diffusivity (RD), is abnormal in TBI patients in these brain regions may provide further insights into the neuropathophysiology in these patients. Therefore, we aimed to assess FA and diffusivity in atlas-based pre-defined brain regions in a series of patients after moderate to severe TBI in order to determine whether microstructural damage occurred more frequently in particular brain regions. Our hypothesis is that the large white matter tracts and deep brain nuclei would be preferentially affected post-TBI regardless of the presence of visible structural injury on conventional structural MRI.

Methods

Participants

Twenty subjects with TBI were recruited from the Neurological Intensive Care Unit (NICU) at the Queen's Medical Center (QMC) in Honolulu, Hawaii. The study was approved by the Institutional Review Board at the QMC, and all TBI subjects had proxy consent provided by their legal guardians. Twenty subjects were enrolled; 3 were excluded because of medical instability that prevented MRI scanning. Seventeen subjects were able to complete MRI scanning, and 2 subjects were excluded from analysis because of imaging artifact. Therefore, fifteen subjects were included in the final imaging analysis. TBI subjects had no pre-existing neurological or psychiatric illness, an admission Glasgow Coma Score (GCS) <13, and were mechanically ventilated and medically stable enough to tolerate MRI within the first 21 days post-injury (mean duration of injury at the time of scan, 10.47 ± 6.77 days). During the brain imaging acquisition, all TBI subjects received mechanical ventilation, were lightly sedated with benzodiazepines and analgesia, and were monitored by the NICU team. Eighteen age- and sex-matched healthy controls without a history of TBI or any chronic medical or neuropsychiatric illnesses were also recruited and studied as comparison subjects.

Image acquisition

A 3.0-Tesla Siemens TIM Trio Scanner (Siemens Medical Solutions, Erlangen, Germany) with a 12-channel head coil was used for all MR scans. The MRI Protocol included a three-plane localizer (repetition time/echo time (TR/TE) = 20/5 ms; 1 average) and a sagittal three-dimensional magnetization-prepared rapid gradient-echo (MP-RAGE) scan (TR/TE/TI [inversion time] = 2200/4.11/1000 ms; 1 average; $208 \times 256 \times 144$ matrix) that was used to assess structural abnormalities. In addition, a fluid-attenuated inversion recovery (FLAIR) scan (TR/TE/TI = 9100/84/2500 ms) was performed for further assessment of gross white matter abnormalities. To evaluate microstructural abnormalities, diffusion measures were obtained using the following parameters: bmax = 1000s/mm^2; 12 directions; TR = 3700 ms; TE = 88 ms; in-plane resolution = 1.7×1.7 mm; and 4 mm axial slices with a 1-mm gap. For each slice, four averages with one additional b = 0 image were acquired. All images were visually inspected to ensure quality of DTI data. Standard quality assurance procedures in DTIStudio (DWI standard deviation maps) were used to identify and eliminate slices and volumes that were affected by motion. All TBI patients were intubated, sedated, and given pharmacological paralysis as needed to avoid head motion artifact. Two of the 17 participants' scans had excess artifacts with distortions on the DTI attributed to large areas of hemorrhage and were not included in the final analyses.

Image processing and diffusion-tensor imaging analysis

DTI data sets were first transferred to DTIStudio (www.MriStudio.org) running on a Windows platform, and motion correction was then performed before calculation of a tensor field as previously described.[10] Using dual-channel large deformation diffeomorphic metric mapping (LDDMM), each tensor field was then transformed to the corresponding JHU-MNI atlas space using a nonlinear transformation process.[11] After the LDDMM registration to a single-subject, skull-stripped MNI atlas, 79 brain regions were automatically segmented in each hemisphere. As previously described, FA, AD (the first eigenvalue), RD (mean of the second and third eigenvalues), and mean diffusivity (MD; mean of the three eigenvalues) were calculated for each participant in each region of interest (ROI) as defined by the JHU-MNI atlas.[10] Preprocessing and quality assessment for the scans were also performed using the Mahalanobis distance, which provides information regarding deviation from the center of the distributions of the variables. This statistical method of using the deviation maps also identified and eliminated slices and volumes that were affected by motion and ensured accurate registration. From the 79 segmented regions, 25 ROIs from the major white matter tracts and subcortical regions were selected from both hemisphere for further analyses. These ROIs were chosen based on the existing literature regarding brain regions affected in patients with TBI.[12–20] These regions include the caudate, putamen, globus pallidus, anterior, superior, and posterior corona radiata, corticospinal tract, superior longitudinal fasciculus, posterior limb and retrolenticular internal capsule, genu, body, and splenium of the corpus callosum, and thalamus (Figs. 1–5).

In total, 11 of the regions had both left and right while the corpus callosum regions had the left and right combined, yielding 25 ROIs measured for MD, but only 17 ROIs were measured for FA, AD, and RD because these three measures are not interpretable in the subcortical gray matter due to the many cross-fibers. However, measures from TBI patients' ROIs that included visible brain lesions were removed from the final analyses for the p values presented in the Results section because blood products can cause DTI signal dropout. The ROIs listed as ''with visible lesions'' in Figures 1–5 are in the same brain region as the visible MRI lesions, but not directly in contused tissue.

Statistical analyses

Statistical analyses were performed using SAS software (9.3; SAS Institute Inc., Cary, NC). Student's t-test or chi-square was used to assess group differences in demographic variables. One-way analyses of covariance (ANCOVA) were utilized to assess

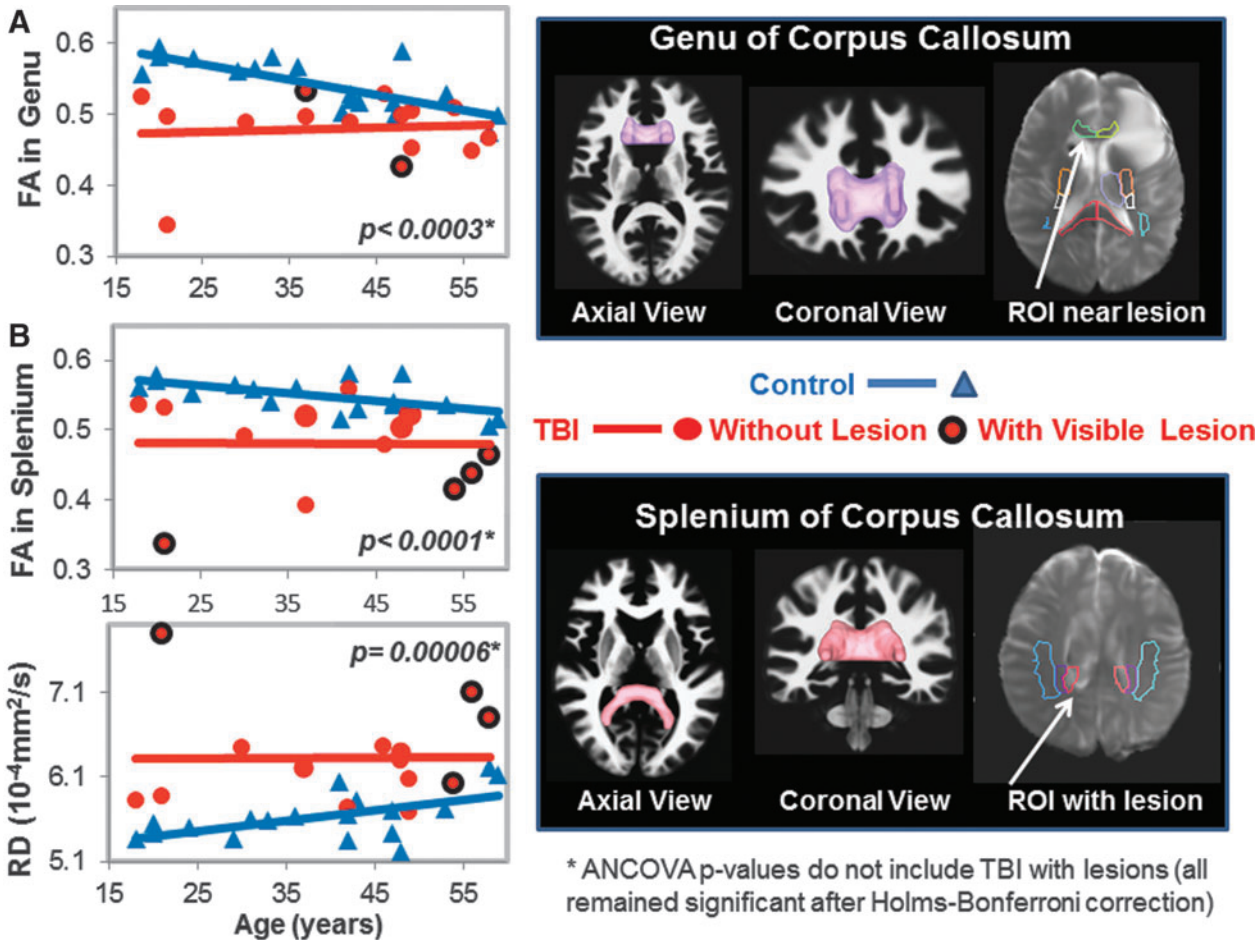

FIG. 1. DTI measures in genu (GCC) and splenium of corpus callosum (SCC). (**A**) Scatter plot shows lower fractional anisotropy (FA) values in the GCC of TBI patients (red dots) compared to controls (blue triangles). Only 2 TBI subjects had visible lesions on MRI (red dots with black outline). The three-dimensional GCC ROI (magenta) used to generate the scatterplot data is shown in the top right panel. A two-dimensional region of interest (ROI; white arrow) showing an adjacent lesion in 1 of the subjects is shown in the B0 image. (**B**) Scatter plots show lower FA values and higher radial diffusivity (RD) values in the SCC in TBI patients compared to controls. Only 4 of the TBI subjects had visible lesions within or near this ROI. The corresponding SCC ROI (pink), along with the projection images of the fiber tracts, and a two-dimensional representation of the ROI (white arrow) shows a lesion within the ROI in 1 of the subjects, are illustrated. See Table 2 and text for corrected p values. ANCOVA, analysis of covariance; DTI, diffusion-tensor imaging; MRI, magnetic resonance imaging; ROI, region of interest; TBI, traumatic brain injury.

group differences in DTI metrics for the selected brain regions between TBI versus control groups. Holms-Bonferroni correction of multiple comparisons[21] was applied for each DTI metric. p values <0.05 that survived Holms-Bonferroni correction were considered statistically significant. Age was included as a covariate because DTI measures change significantly with age.[22] Specifically, regional FA has been demonstrated to decline in a predictable fashion in association with normal aging.[23] Therefore, control subjects were carefully age matched as represented in Figures 1–5. Additionally, Shapiro-Wilk tests were used to evaluate the normality of DTI measures in each ROIs that showed group differences, separately for TBI and control subjects. For measures that deviated from normality, nonparametric Kruskal-Wallis tests were used to confirm ANCOVA results (group differences).

Results

Participant characteristics

Healthy controls and TBI subjects with usable DTI scans did not differ in age (controls, 38.97 ± 3.04 years; TBI participants, 39.29 ± 3.23 years; $p = 0.94$), sex proportion (13 [72%] male controls, 12 [71%] male TBI participants; $p = 0.91$), or percentage of individuals who tested positive for methamphetamine (controls, 4 of 18 [22%], TBI, 7 of 17 [41%]; $p = 0.33$; Table 1). All TBI subjects sustained a blunt force TBI, with mean GCS after stabilization of 6.47 ± 1.51 with a range of 3–9, and were scanned 10.47 ± 6.77 days post-injury. Head computed tomography (CT) scans were performed upon admission and rated using the Marshall Score.[24] Subsequent MRI scanning demonstrated structural brain injury (parenchymal contusion, subdural hematoma, traumatic subarachnoid hemorrhage, and white matter hyperintensity) was visible on T1 and T2 MRI sequences in the left hemisphere in 6 (35%), the right hemisphere in 5 (30%), and bilaterally in 6 (35%) TBI subjects. Contusions were observed in the left hemisphere in 6 (35%), the right hemisphere in 2 (12%), and bilaterally in 5 (29%) TBI subjects. Subdural hematoma was observed in the left hemisphere in 1 (5%), right hemisphere in 3 (18%), and bilaterally in 3 (18%) participants. Bilateral traumatic subarachnoid hemorrhage was observed in 3 subjects (18%), whereas white matter hyperintensities were located in the corpus callosum,

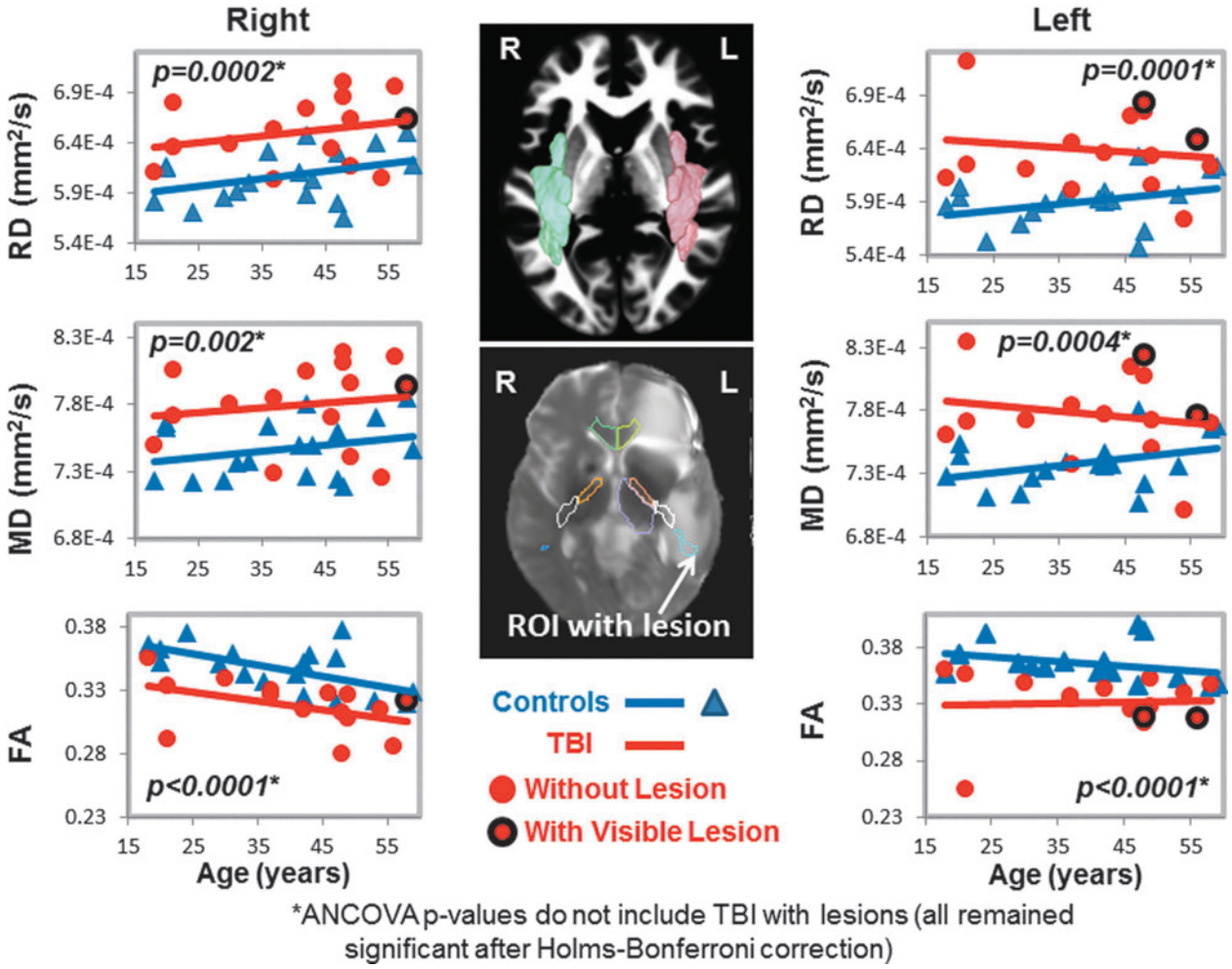

FIG. 2. DTI measures in bilateral superior longitudinal fasciculus (SLF). Scatter plots show higher RD and MD, as well as lower FA in the SLF bilaterally, in TBI patients (red dots) compared to controls (blue triangles). In the SLF, only 2 TBI patients had lesions (red dots with black outline) in the left hemisphere (plots on the left), and only 1 TBI patient had a lesion in the right hemisphere (plots on the right). The volumetric representation of the left (pink) and right (green) SLF ROIs are shown in the top panel, and a two-dimensional representation of the ROI is shown including a lesion in the bottom panel (white arrow). See Table 2 and text for corrected *p* values. ANCOVA, analysis of covariance; DTI, diffusion-tensor imaging; FA, fractional anisotropy; MD, mean diffusivity; RD, radial diffusivity; ROI, region of interest; TBI, traumatic brain injury.

internal capsule, and the superior longitudinal fasciculus on FLAIR imaging in 7 (41%) of the TBI subjects (some of these lesions are illustrated in Figs. 1–4).

Diffusion-tensor imaging measures

Two of the 17 participants' DTI scans could not be registered accurately to the automated atlas because of hemorrhage-associated artifacts that led to image distortion. In the remainder 15 participants, half (7 of 14) of the brain regions, including nine ROIs, with normal appearing white matter showed significant group differences on DTI measures (FA, RD, or MD) compared to noninjured subjects (Table 2; Figs. 1–5). TBI subjects had lower FA values than controls in the corpus callosum (genu, FA p-corrected = 0.02; splenium FA, p-corrected = 0.015; Fig. 1A,B), superior longitudinal fasciculus (left FA, p-corrected = 0.007; right FA, p-corrected = 0.004; Fig. 2), and internal capsule (posterior limb: left FA, p-corrected = 0.008; right FA, p-corrected = 0.004; retrolenticular: right FA, $p = 0.04$; Fig. 3A,B). Higher radial or mean diffusion measures were also observed in TBI relative to control subjects in the corpus callosum (splenium RD, p-corrected = 0.007; Fig. 1B), superior longitudinal fasciculus (left RD, p-corrected = 0.01; left MD, $p = 0.04$; right RD, p-corrected = 0.01; Fig. 2), right retrolenticular internal capsule (RD, p-corrected = 0.0006; MD, p-corrected = 0.02; Fig. 3B), posterior corona radiata (left RD, corrected $p = 0.002$; left MD, corrected $p = 0.007$; right RD, corrected $p = 0.009$, right MD, corrected $p = 0.02$; Fig. 4), and thalamus (left MD, corrected $p < 0.007$; Fig. 5). No group differences were found on axial diffusion in any of these brain regions.

In the TBI group, four measures deviated from normality (FA in the genu of the corpus callosum, MD in the right retrolenticular internal capsule, RD in the right retrolenticular internal capsule, and FA in the left superior longitudinal fasciculus). However, the group differences in these four measures remained significant ($p < 0.05$) when data were analyzed with nonparametric procedures (Kruskal-Wallis tests).

Only a few lesions were observed within the ROIs of TBI patients containing significant group differences between TBI

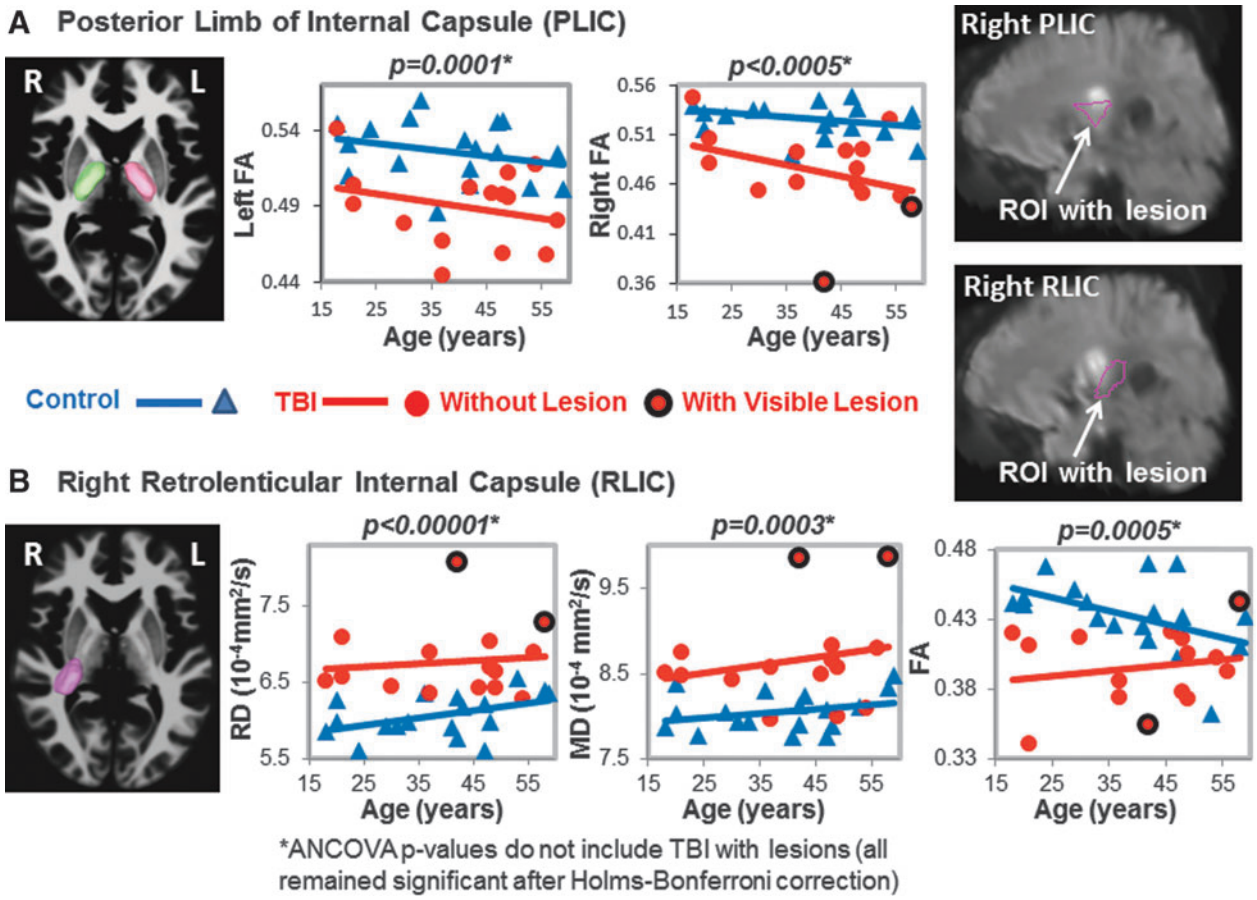

FIG. 3. DTI Measures in posterior limb (PLIC) and retrolenticular internal capsule (RLIC). (**A**) PLIC: The left (pink) and right (green) three-dimensional ROIs are shown in the left panel. The corresponding scatter plots show lower FA values in TBI patients (red dots) compared to controls (blue triangles) in both hemispheres. Two of the TBI patients showed lesions within the right PLIC (red dots with black outline), as shown in the upper right panel. (**B**) RLIC: The three-dimensional ROI (pink) is illustrated on an axial MRI. The scatter plots show higher RD and MD and lower FA in TBI patients compared to controls. Only 2 TBI subjects had lesions within this ROI (white arrow in MRI). See Table 2 and text for corrected *p* values. ANCOVA, analysis of covariance; DTI, diffusion-tensor imaging; FA, fractional anisotropy; MD, mean diffusivity; MRI, magnetic resonance imaging; RD, radial diffusivity; ROI, region of interest; TBI, traumatic brain injury.

patients and controls. These lesions are illustrated in the scatter plots to show the DTI measures in these ROIs with lesions, but they were not included in the statistical analyses. In the corpus callosum, 2 of 15 patients had visible lesions in the genu (Fig. 1A), and 4 of 15 had visible lesions in the splenium (Fig. 1B). In the superior longitudinal fasciculus, 2 of 15 TBI patients had lesions in the left hemisphere, and 1 of 15 patients had a lesion in the right hemisphere (Fig. 2). In the internal capsule, 2 of 15 subjects had lesions in the right posterior limb (Fig. 3A), and these same 2 patients also had lesions in the right retrolenticular region. In the left retrolenticular region, 1 of 15 patients had a lesion within the ROI (Fig. 3B). In the posterior corona radiata, 2 of 15 subjects had lesions within the ROI in the left hemisphere, and no lesions were observed in the right hemisphere (Fig. 4). No lesions were observed in TBI patients in the thalamus, but significantly higher MD values were observed in TBI relative to control subjects (Fig. 5).

None of these abnormal DTI metrics correlated with the GCS on admission or with time between injury and MRI scanning in these participants. Further, the DTI metrics that showed group differences in TBI participants also did not correlate with the Glasgow Outcome Scale-Extended at 6 months in these subjects.

Discussion

This prospective case-control study of DTI with quantitative analysis in multiple brain regions in subjects with acute moderate to severe TBI has two main findings. First, subjects with acute moderate and severe TBI had microstructural damage in five important brain regions, including the corpus callosum, superior longitudinal fasciculus, posterior corona radiata, internal capsule, and thalamus. Among these brain regions, the large and long white matter tracts are essential for frontal and parietal lobe interhemispheric and intrahemispheric connectivity. We did not find significant correlation with clinical outcome on the Glasgow Outcome Scale at 6 months; this is most likely because of the small sample size in this study. Alternatively, more detailed neuropsychological tests to evaluate executive function and sensorimotor function may be needed to evaluate for possible functional deficits associated with these brain regions. Additionally, if no correlations were observed between the DTI abnormalities and cognitive outcomes, these findings may reflect reversible brain edema in these brain regions in this early stage of moderate to severe TBI. Second, most of the subjects showed abnormal diffusivity in multiple, but selected, brain regions,

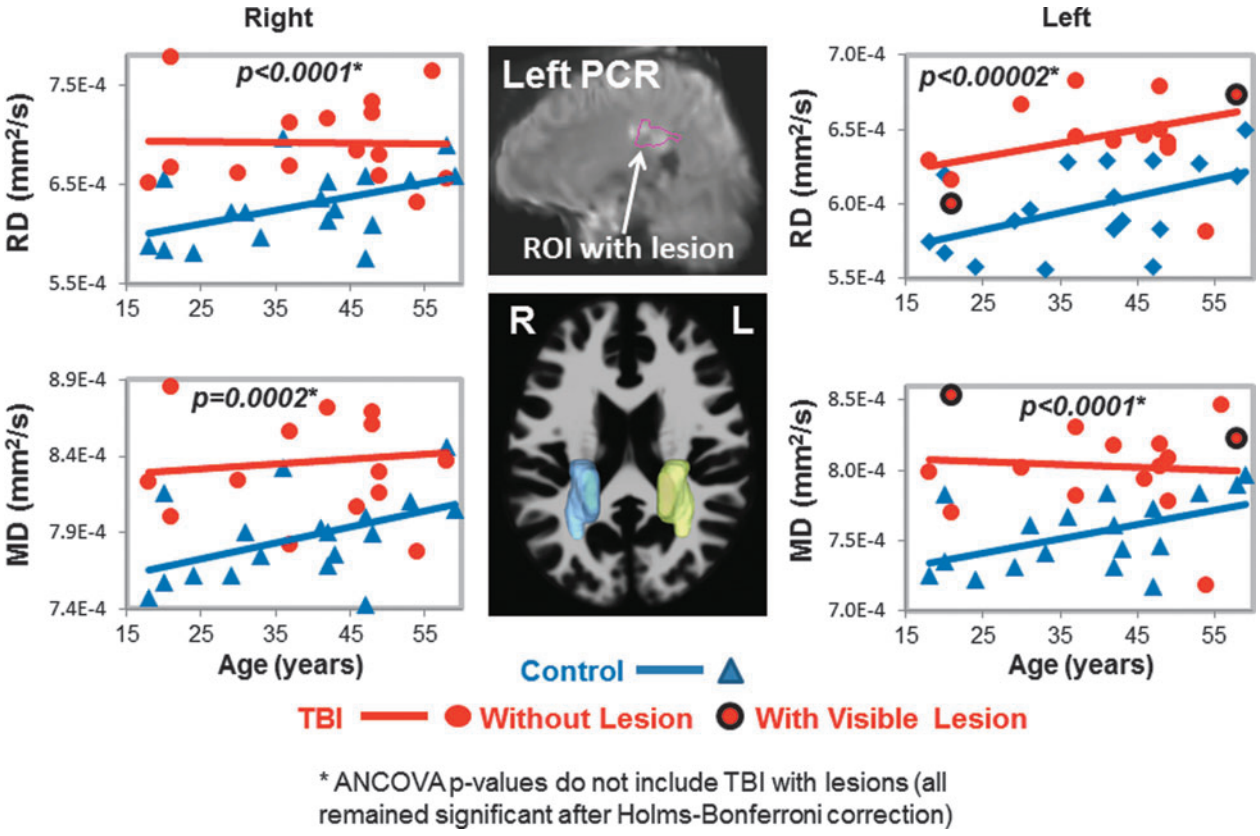

FIG. 4. Radial and mean diffusivities in posterior corona radiata (PCR). Scatter plots show higher RD and MD values in TBI patients (red dots) compared to controls (blue triangles) bilaterally. Only 2 TBI patients had lesions within the left PCR (red dots with black outline in scatterplots, and white arrow, top middle MRI). Three-dimensional representations of the left (yellow) and right (blue) PCR ROIs are shown on an axial MRI (middle bottom panel). See Table 2 and text for corrected *p* values. ANCOVA, analysis of covariance; MD, mean diffusivity; MRI, magnetic resonance imaging; RD, radial diffusivity; ROI, region of interest; TBI, traumatic brain injury.

including brain regions with and without visible abnormalities on the regular structural MRI. These findings demonstrate the heterogeneous and extensive microstructural abnormalities in patients with TBI. These findings also illustrate the greater sensitivity of DTI compared to conventional structural MRI in detecting microstructural abnormalities in patients with TBI.

Our study found abnormal regional fractional anisotropy in specific brain regions even in the absence of visible brain lesions. This is in contrast to a recent study of patients with acute mild TBI, which found DTI abnormalities in areas with traumatic intracranial lesions on traditional MRI or CT imaging, but not in those with normal early brain imaging.[25] Thus, the severity of injury may

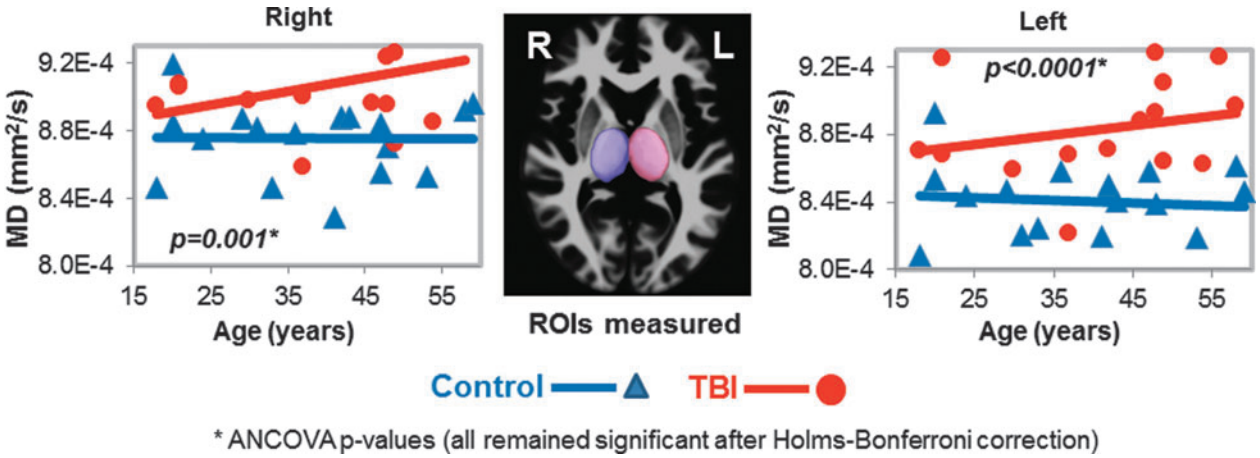

FIG. 5. Higher mean diffusivities in thalamus of TBI patients. Scatter plots show higher MD values in both thalamus of TBI patients (red dots) compared to controls (blue triangles); however, only the left thalamic MD remained significant after Bonferroni corrections. The three-dimensional ROIs for the thalamus from these ROIs are shown in the images (middle panel). See Table 2 and text for corrected *p* values. ANCOVA, analysis of covariance; MD, mean diffusivity; ROI, region of interest; TBI, traumatic brain injury.

Table 1. Clinical Data for All TBI Subjects on Admission and Glasgow Outcome Scale at 6 Months

TBI patient no.	*Age (years)*	*Sex*	*Glasgow Coma Scale on admission*	*Marshal CT classification*	*Time to MRI scan (days)*	*Lesion side location*	*Lesion type*				*Glasgow Outcome Scale-Extended at 6 months*
							Subdural hematoma	*Contusion*	*Traumatic subarachnoid hemorrhage*	*White matter hyperintensities*	
1	58	Male	9	DI II	7	Bilateral frontal	Bilateral	Bilateral			3
2	33	Male	5	EML	4	Left fronto-temporal	Left	Left			5
3	37	Male	3	DI II	2	Left frontal		Left	Bilateral		ND
4	42	Male	5	DI II	3	Right basal ganglia			Bilateral	Right CSO	6
5	21	Female	7	DI II	10	Right		Right			6
6	56	Female	6	DI II	11	Bilateral		Bilateral			5
7	48	Male	7	DI II	17	Left		Left		Brainstem	3
8	21	Male	7	DI III	17	Right	Right	Right		Bifrontal	7
9	48	Male	6	DI II	4	Left frontal		Left			4
10	46	Male	8	DI III	18	Bilateral temporal, left parietal		Bilateral temporal, left parietal			5
11	30	Female	8	DI III	27	Left basal ganglia				Left CSO	4
12	49	Female	5	DI II	4	Bilateral frontal			Bilateral	Bifrontal	5
13	49	Female	7	DI III	10	Bilateral frontal	Bilateral	Bilateral			4
14	18	Male	7	DI II	11	Right temporal	Right				5
15	37	Male	5	DI II	10	Bilateral		Bilateral Frontal		Left basal Ganglia; brainstem	3
16	21	Male	7	DI II	15	Left temporal	Bilateral	Left			ND
17	54	Male	7	DI III	8	Right frontal	Right			Bifrontal; corpus callosum	1

TBI, traumatic brain injury; CT, computed tomography; MRI, magnetic resonance imaging; ND, not done; R, right; L, left; B, bilateral; CSO, centrum semiovale; DI II, diffuse injury type II; DI III, diffuse injury type III; EML, evacuated mass lesion.

Table 2. Fractional Anisotropy (FA) and Diffusivity in Different Brain Regions (Mean ± SE) of TBI Subjects and Controls

	TBI subjects (n = 15)		*Controls (n = 18)*		*TBI vs. controls ANCOVA-corr-p value (left)*	*TBI vs. controls ANCOVA-corr-p value (right)*
Brain region	*Left*	*Right*	*Left*	*Right*		
Fractional anisotropy (FA)						
Anterior corona radiata (ACR)	0.315 ± 0.010	0.332 ± 0.008	0.345 ± 0.007	0.366 ± 0.006	0.99	0.99
Superior corona radiata (SCR)	0.345 ± 0.006	0.335 ± 0.007	0.364 ± 0.005	0.365 ± 0.005	0.99	0.10
Posterior corona radiata (PCR)	0.338 ± 0.006	0.324 ± 0.010	0.368 ± 0.005	0.360 ± 0.007	0.09	0.56
Corticospinal tract	0.347 ± 0.009	0.346 ± 0.009	0.363 ± 0.007	0.356 ± 0.009	0.99	0.99
Superior longitudinal fasciculus (SLF)	0.332 ± 0.007	0.318 ± 0.005	0.366 ± 0.004	0.347 ± 0.004	**0.007**	**0.004**
Posterior limb internal capsule (PLIC)	0.490 ± 0.007	0.472 ± 0.011	0.526 ± 0.005	0.527 ± 0.005	**0.008**	**0.004**
Retrolenticular IC	0.388 ± 0.006	0.396 ± 0.007	0.411 ± 0.005	0.433 ± 0.006	0.50	**0.04**
Genu of corpus callosum (CC)	0.480 ± 0.014		0.542 ± 0.009		**0.02**	
Body of CC	0.400 ± 0.017		0.467 ± 0.010		0.08	
Splenium of CC	0.481 ± 0.016		0.549 ± 0.006		**0.015**	
Radial diffusivity (RD)						
Anterior corona radiata (ACR)	6.93 ± 0.264	6.52 ± 0.096	6.26 ± 0.077	6.09 ± 0.072	0.99	0.07
Superior corona radiata (SCR)	6.02 ± 0.099	6.14 ± 0.105	5.72 ± 0.047	5.75 ± 0.056	0.63	0.14
Posterior corona radiata (PCR)	6.53 ± 0.085	6.92 ± 0.111	5.98 ± 0.069	6.29 ± 0.086	**0.002**	**0.009**
Corticospinal tract	6.47 ± 0.088	6.43 ± 0.117	6.65 ± 0.126	6.59 ± 0.145	0.99	0.99
Superior longitudinal fasciculus (SLF)	6.38 ± 0.096	6.51 ± 0.085	5.91 ± 0.053	6.07 ± 0.061	**0.01**	**0.01**
Posterior limb internal capsule (PLIC)	5.09 ± 0.078	5.41 ± 0.168	4.78 ± 0.057	4.85 ± 0.048	0.35	0.19
Retrolenticular IC	6.39 ± 0.077	6.77 ± 0.120	6.07 ± 0.062	6.06 ± 0.065	0.27	**0.0006**
Genu of corpus callosum (CC)	6.33 ± 0.163		5.67 ± 0.099		**0.05**	
Body of CC	7.25 ± 0.228		6.79 ± 0.120		0.99	
Splenium of CC	6.33 ± 0.147		5.63 ± 0.067		**0.007**	
Mean diffusivity (MD)						
Anterior corona radiata (ACR)	8.39 ± 0.250	8.00 ± 0.095	7.80 ± 0.058	7.71 ± 0.057	0.99	0.99
Superior corona radiata (SCR)	7.41 ± 0.106	7.50 ± 0.114	7.15 ± 0.044	7.21 ± 0.051	0.99	0.99
Posterior corona radiata (PCR)	8.03 ± 0.086	8.37 ± 0.111	7.55 ± 0.061	7.87 ± 0.067	**0.007**	**0.02**
Corticospinal tract	7.96 ± 0.085	7.91 ± 0.112	8.33 ± 0.125	8.20 ± 0.138	0.99	0.99
Superior longitudinal fasciculus (SLF)	7.77 ± 0.088	7.80 ± 0.081	7.38 ± 0.047	7.47 ± 0.050	**0.04**	0.13
Posterior limb internal capsule (PLIC)	7.28 ± 0.080	7.58 ± 0.149	7.14 ± 0.051	7.26 ± 0.044	0.99	0.99
Retrolenticular IC	8.15 ± 0.082	8.66 ± 0.144	7.93 ± 0.049	8.05 ± 0.052	0.99	**0.02**
Caudate	9.22 ± 0.133	9.29 ± 0.178	8.66 ± 0.105	8.91 ± 0.102	0.07	0.99
Putamen	7.85 ± 0.151	7.80 ± 0.174	7.49 ± 0.087	7.23 ± 0.078	0.99	0.35
Globus pallidus	8.40 ± 0.215	8.69 ± 0.293	8.07 ± 0.087	8.07 ± 0.100	0.99	0.99
Thalamus	8.83 ± 0.078	9.08 ± 0.076	8.41 ± 0.053	8.76 ± 0.052	**0.007**	0.12
Genu of corpus callosum (CC)	9.01 ± 0.130		8.72 ± 0.069		0.99	
Body of CC	9.51 ± 0.196		9.50 ± 0.078		0.99	
Splenium of CC	9.00 ± 0.141		8.72 ± 0.058		0.99	

ANCOVA, analysis of covariance; TBI, traumatic brain injury.

impact decisions regarding the specific modality of advanced MRI best suited to determine extent of intracranial injury.

We found consistently lower FA, indicating abnormal axonal integrity, in multiple regions that included white matter tracts that connect the frontal lobes (Figs. 1 and 2) and involved in motor function (Fig. 3) in the acute stages, post-moderate to severe TBI. These findings are consistent with the lower FA found in past studies in patients with acute mild TBI,[26,27] as well as more chronic stages post-TBI.[28] In our TBI patients who required NICU care, this diffuse pattern of involvement in half of the large white matter tracts was present both in brain regions with and without visible structural abnormalities on conventional structural MRI. White matter disruption was previously shown to be poorly estimated by conventional imaging even when specialized MRI sequences such as susceptibility weighted images (SWIs) are used. SWI imaging can be used to detect traumatic microbleeds and is used as a method for measuring indirect evaluation of axonal damage in the clinical environment. However, previous studies have predominantly been performed in the chronic stages post-TBI. [30,31]

As expected, mean diffusivity was greater than normal, attributed primarily to the greater radial diffusivity, in these large and long white matter tracts (i.e., posterior coronal radiata and superior longitudinal fasciculus) of TBI subjects, which is consistent with past findings in the pediatric and adult populations in the subacute to chronic stages post-TBI.[29,32] The higher radial diffusivity likely reflects the subacute neuroinflammation, with greater water content

associated with edema between the myelin sheaths, followed by a complex process of continued degeneration and regional repair.[33,34] Additionally, the MD was significantly greater than normal in the left thalamus, which is consistent with the finding of abnormal resting state functional MRI connectivity found between thalamus and cortex in subjects with moderate to severe TBI.[35] Together with these past studies, the abnormal thalamic diffusivity indicate deep gray matter injury, which might have resulted from torsional forces associated with TBI on these centrally located deep structures.

As expected, the affected brain regions in this study are mostly consistent with those found in subjects across a spectrum of TBI acuity and severity.[5,26,28,34,36–39] We found lower FA and greater than normal MDs and RDs in these brain regions, but no significant abnormalities in axial diffusivity in any brain regions. Overall, although we assessed for group differences in 14 brain regions (11 had right and left, plus three corpus callosum regions) for a total of 25 ROIs measured, only nine ROIs showed significant group differences (on corrected *p* values) on various DTI metrics (FA, RD, or MD); see Table 2. Therefore, 16 ROIs showed no group differences between the controls and the TBI patients. These relatively normal brain regions in the TBI patients include the shorter white matter tracts (anterior corona radiata, superior corona radiata) and the striatal structures (caudate, putamen, and globus pallidus), which may be less susceptible to torsional forces that occur with TBI. These findings suggest that the microstructural brain injuries are not completely diffuse throughout the brain; however, the lack of group differences may also be attributed to the relatively small sample size for our subject groups and the possibly smaller effect size in these other brain regions.

The absence of abnormalities in axial diffusivity was also reported previously in the corpus callosum of patients with TBI.[40] However, some of these abnormalities in the DTI metrics may vary depending on when the DTI was performed after the TBI, given that reactive inflammation and microstructural integrity changes dynamically over time.[41,42] Similarly, FA showed dynamic changes over time, with increases over the first 2 weeks and decreases between 3 and 6 months post-TBI.[27] However, our patients already showed lower than normal FA, suggesting decreased axonal integrity, within the first 3 weeks of acute TBI. This early microstructural injury has been demonstrated to correlate with the presence of tau protein and microfilament in the extracellular fluid in microdialysis studies.[43] These early changes in FA may reflect severe brain injuries in our patients, given that microstructural integrity varies with injury severity.[29] However, our abnormal DTI metrics did not correlate with the Glasgow Outcome Scales at 6 months in these TBI patients. Therefore, these early changes in FA also could reflect brain edema. More accurate interpretation of these findings would require longitudinal follow-up studies with both DTI and more detailed clinical assessments. These findings highlight the importance of considering both temporal variables and the brain injury severity when interpreting DTI metrics after brain injury.

Nevertheless, our findings are clinically significant because diffusion metrics have been shown to be related to, and likely predictive of, outcome including mortality[44] as well as cognitive and motor performance on neuropsychological testing.[28,42–47] Similar changes in DTI measures are also associated with mood disorders[48] and deficits in learning ability[49] post-TBI. Further, the diffuse white matter injury is typically not readily apparent with conventional structural MRI that is often used for prognostication post-TBI. In the current study, visible lesions were only observed in a minority of affected regions, and TBI patients with lesions within the significant ROI did not always have the most aberrant values. Our study provides further evidence that brain injury associated with TBI may be apparent only on DTI measures.[50,51] Thus, DTI is a useful and sensitive imaging modality to detect microstructural brain injury even in normal appearing brain regions.

Our study has several limitations. First, microstructural abnormalities are dynamic and change over time post-TBI, and although all imaging was done subacutely within the first 3 weeks post-injury, the scans were performed on different post-injury days. Second, because the effects of TBI during the chronic phase are not the same as those observed during the acute phase of TBI,[52] and the manner in which the changes correlate with functional outcomes is also dependent upon the time of assessment,[14] future studies with longitudinal assessments at later time points are needed to better determine whether these early microstructural abnormalities can predict clinical outcomes. Third, the DTI sequence used in the current study has only 12 diffusion directions, and involved non-isotropic voxels, which may have increased the potential for partial volume effects and thus decreased the accuracy of FA and diffusivity measures. However, similar limitations are commonly encountered in the clinical environment, which may make our results more applicable clinically. Fourth, because of the relatively small sample size, some of the ROIs that had small effect size, even if diffuse microstructural brain injury was present, may not show group differences. Last, our relatively small sample size also did not allow us to adequately correlate the findings with clinical outcomes or evaluate the possible sex-differences or other comorbid issues (e.g., other substances use) in our TBI subjects.

In conclusion, this study demonstrates the multiple regional DTI abnormalities, including abnormal axonal integrity and neuroinflammation, primarily involving long white matter tracts within the first few weeks after moderate to severe brain injury. These abnormalities are located in brain regions that will likely impact long-term recovery of cognition and motor function post-TBI. DTI is a sensitive and useful tool for detecting microstructural abnormalities even in normal-appearing brain regions on conventional MRI.

Acknowledgments

The authors thank David Greenstein, BS, for image processing, Kenichi Oishi, MD, PhD, for supervision and guidance in the use of DTIStudio, and Katherine Denny, PhD, for data analysis and manuscript editing.

This work was funded by 1R03DA024199 (KO) and K24-DA16170 (LC).

Author Disclosure Statement

No competing financial interests exist.

References

1. Bruns, J., and Hauser, W.A. (2003). The epidemiology of traumatic brain injury: a review. Epilepsia 44, 2–10.
2. Wu, H.-M., Huang, S.-C., Hattori, N., Glenn, T.C., Vespa, P.M., Yu, C.-L., Hovda, D.A., Phelps, M.E., and Bergsneider, M. (2004). Selective metabolic reduction in gray matter acutely following human traumatic brain injury. J. Neurotrauma, 21, 149–161.
3. Vespa, P.M., O'Phelan, K., McArthur, D., Miller, C., Eliseo, M., Hirt, D., Glenn, T., and Hovda, D.A. (2007). Pericontusional brain tissue exhibits persistent elevation of lactate/pyruvate ratio independent of cerebral perfusion pressure. Crit. Care Med. 35, 1153–1160.

4. Dodd, A.B., Epstein, K., Ling, J.M., and Mayer, A.R. (2014). Diffusion tensor imaging findings in semi-acute mild traumatic brain injury. J. Neurotrauma 31, 1235–1248.
5. Xiong, K., Zhu, Y., and Zhang, W. (2014). Diffusion tensor imaging and magnetic resonance spectroscopy in traumatic brain injury: a review of recent literature. Brain Imaging Behav. 8, 487–496.
6. Hulkower M.B., Poliak, D.B., Rosenbaum, S.B., Zimmerman, M.E., and Lipton, M.L. (2013). A decade of DTI in traumatic brain injury: 10 years and 100 articles later. Am. J. Neuroradiol. 34, 2064–2074.
7. Newcombe, V., Chatfield, D., Outtrim, J., Vowler, S., Manktelow, A., Cross, J., Scoffings, D., Coleman, M., Hutchinson, P., Coles, J., Carpenter, T.A., Pickard, J., Williams, G., and Menon, D. (2011). Mapping traumatic axonal injury using diffusion tensor imaging: correlations with functional outcome. PLoS One 6, e19214.
8. Galanaud, D., Perlbarg, V., Gupta, R., Stevens, R.D., Sanchez, P., Tollard, E., de Champfleur, N.M., Dinkel, J., Faivre, S., Soto-Ares, G., Veber, B., Cottenceau, V., Masson, F., Tourdias, T., André, E., Audibert, G., Schmitt, E., Ibarrola, D., Dailler, F., Vanhaudenhuyse, A., Tshibanda, L., Payen, J.F., Le Bas, J.F., Krainik, A., Bruder, N., Girard, N., Laureys, S., Benali, H., and Puybasset, L.; Neuro Imaging for Coma Emergence and Recovery Consortium. (2012). Assessment of white matter injury and outcome in severe brain trauma: a prospective multicenter cohort. Anesthesiology 117, 1300–1310.
9. Kim, J., Parker, D., Whyte, J., Hart, T., Pluta, J., Ingalhalikar, M., Coslet, H.B., and Verma, R. (2014). Disrupted structural connectome is associated with both psychometric and real world neuropsychological impairment in diffuse traumatic brain injury. J. Int. Neuropsychol. Soc. 20, 887–896.
10. Jiang, H., van Zijl, P.C., Kim, J., Pearlson, G.D., Mori, S. (2006) DtiStudio: resource program for diffusion tensor computation and fiber bundle tracking. Comput. Methods Programs Biomed. 81, 106–116.
11. Ceritoglu, C., Oishi, K., Li, X., Chou, M.C., Younes, L., Albert, M., Lyketsos, C., vanZijl, P.C., Miller, M.I., and Mori, S. (2009). Multi-contrast large deformation diffeomorphic metric mapping for diffusion tensor imaging. Neuroimage 47, 618–627.
12. Herrerra, J.J., Bockhorst, K., Kondraganti, S., Stertz, L., Quevedo, J., Narayana, and P.A. (2016). Acute white matter damage after frontal mild traumatic brain injury. J. Neurotrauma 43, 291–299.
13. Edlow, B.L., Copen, W.A., Izzy, S., Bakhadirov, K., van der Kouwe, A., Glenn, M.B., Greenberg, S.M., Greer, D.M., and Wu, O. (2016). Diffusion tensor imaging in acute-to-subacute traumatic brain injury: a longitudinal analysis. BMC Neurol. 16, 2.
14. Babcock, L., Yuan, W., Leach, J., Nash, T., and Wade, S. (2015). White matter alterations in youth with acute mild traumatic brain injury. J. Pediatr. Rehabil. Med. 8, 285–296.
15. D'Souza, M.M., Trivedi, R., Singh, K., Grover, H., Choudhury, A., Kaur, P., Kumar, P., and Tripathi, R.P. (2015). Traumatic brain injury and the post-concussion syndrome: A diffusion tensor tractography study. Indian J. Radiol. Imaging 25, 404–414.
16. Kamnaksh, A., Budde, M.D., Kovesdi, E., Long, J.B., Frank, J.A., and Agoston, D.V. (2014). Diffusion tensor imaging reveals acute subcortical changes after mild blast-induced traumatic brain injury. Sci. Rep. 4, 4809.
17. Narayana, P.A., Yu, X., Hasan, K.M., Wilde, E.A., Levin, H.S., Hunter, J.V., Miller, E.R., Patel, V.K., Robertson, C.S., and McCarthy, J.J. (2014). Multi-modal MRI of mild traumatic brain injury. Neuroimage Clin. 7, 87–97.
18. Kasahara, K., Hashimoto, K., Abo, M., and Senoo, A. (2012). Voxel- and atlas-based analysis of diffusion tensor imaging may reveal focal axonal injuries in mild traumatic brain injury—comparison with diffuse axonal injury. Magn. Reson. Imaging, 30, 496–505.
19. Chu, Z., Wilde, E.A., Hunter, J.V., McCauley, S.R., Bigler, E.D., Troyanskaya, M., Yallampalli, R., Chia, J.M., and Levin, H.S. (2010). Voxel-based analysis of diffusion tensor imaging in mild traumatic brain injury in adolescents. Am. J. Neuroradiol. 31, 340–346.
20. Holm, S. (1979). A simple sequentially rejective multiple test procedure. Scand. J. Stat. 6, 65–70.
21. Rabinowitz, A.R., and Levin, H.S. (2014). Cognitive sequelae of traumatic brain injury, in: *Neuropsychiatry of Traumatic Brain Injury, An Issue of Psychiatric Clinics of North America*. R.E. Jorge and D.B. Arciniegas(eds). Elsevier Health Sciences: Philadelphia, PA, pps. 1–12.
22. DeGroot, M., Cremers, L.G., Ikram, M.A., Hofman, A, Krestin, G.P., van der Lugt, A., Neissen, W.J., Vernooij, M.W. (2016). White matter degeneration with aging: longitudinal diffusion MR imaging analysis. Radiology 279, 532–541.
23. Yang, A.C., Tsai, S.-J., Liu, M.-E., Huang, C.-C., Lin, C.-P. (2016). The association of aging with white matter integrity and functional connectivity hubs. Front. Aging Neurosci. 8, 143.
24. Marshall, L.F., Bowers, M.S., Klauber, M.R., van Berkum, C.M., Eisenberg, H.M., Jane, J.A., Luerssen, T.G., Marmarou, A., and Foulkes, MA. (1991). A new classification of head injury based on computerized tomography. J. Neurosurg. 75, S14–S17.
25. Yuh, E.L., Cooper, S.R., Mukherjee, P., Yue, J.K, Lingsma, H.F., Gordon, W.A., Valadka, A.B., Okonkwo, D.O., Schnyer, D.M., Vassar, M.J., Maas, A.I.R., and Manley, G.T. (2014). Diffusion Tensor Imaging for Outcome Prediction in Mild Traumatic Brain Injury: a TRACK-TBI study. J. Neurotrauma 31, 1457–1477.
26. Matsushita, M., Hosoda, K., Naitoh, Y., Yamashita, H., and Kohmura, E.K. (2011). Utility of diffusion tensor imaging in the acute stage of mild to moderate traumatic brain injury for detecting white matter lesions and predicting long-term cognitive function in adults. J. Neurosurg. 115, 130–139.
27. Lipton, M.L., Kim, N., Park, Y.K., Hulkower, M.B., Gardin, T.M., Shifteh, K., Kim, M., Zimmerman, M.E., Lipton, R. B., and Branch, C. A. (2012). Robust detection of traumatic axonal injury in individual mild traumatic brain injury patients: intersubject variation, change over time and bidirectional changes in anisotropy. Brain Imaging Behav. 6, 329–342.
28. Kraus, M.F., Susmaras, T., Caughlin, B.P., Walker, C.J., Sweeney, J.A., and Little, D.M. (2007). White matter integrity and cognition in chronic traumatic brain injury: a diffusion tensor imaging study. Brain 130, 2508–2519.
29. Genc, S., Anderson, V., Ryan, N.P., Malpas, C.B., Catroppa, C., Beauchamps, M.H., and Silk, T.J. (2016). Recovery of white matter following pediatric traumatic brain injury depends on injury severity. J. Neurotrauma. 33, 1–9.
30. Zappala, G., Thiebaut de Schotten, M., and Eslinger, P.J. (2012). Traumatic brain injury and the frontal lobes: What can we gain with diffusion tensor imaging? Cortex 48, 156–165.
31. Toth, A., Kornyei, B., Kovacs, N., Rostas, T., Buki, A., Doczi, T., Bogner, P., and Schwarcz, A. (2018). Both hemorrhagic and non-hemorrhagic traumatic MRI lesions are associated with the microstructural damage of the normal appearing white matter. Behav. Brain Res. 340, 106–116.
32. Wilde, E.A., Li, X., Hunter, J.V., Narayana, P.A., Hasan, K., Biekman, B., Swank, P., Robertson, C., Miller, E., McCauley, S.R., Chu, Z.D., Faber, J., McCarthy, J., and Levin, H.S. (2016). Loss of consciousness is Related to white Matter Injury in Mild Traumatic Brain Injury. J. Neurotrauma 33, 2000–2010.
33. Rubovitch, V., Ten-Bosch, M., Zohar, O., Harrrison, C.R., Tempel-Brami, C., Stein, E., Hoffer, B.J., Balaban, C.D., Schreiber, S., Chiu, W.T., and Pick, C.G. (2011). A mouse model of blast induced mild traumatic brain injury. Exp. Neurol. 323, 280–289.
34. Sidaros, A., Engberg, A.W., Sidaros, K., Liptrot, M.G., Herning, M., Petersen, P., Paulson O.B., Jernigen, T.L., and Rostrup, E. (2008). Diffusion tensor imaging during recovery from severe traumatic brain injury and relation to clinical outcome: a longitudinal study. Brain 131, 559–572.
35. Tang, L., Ge, Y., Sodickson, D.K., Miles, L., Zhou, Y., Reaume, J., and Grossman, R.I. (2011). Thalamic resting-state functional networks: disruption in patients with mild traumatic brain injury. Radiology 260, 831–840.
36. Meythaler, J.M., Peduzzi, J.D., Eleftheriou, E., and Novak, T.A. (2001). Current concepts: diffuse axonal injury-associated traumatic brain injury. Arch. Phys. Med. Rehabil. 82, 1461–1471.
37. Salmond, C.H., Menon, D.K., Chatfield, D.A., Williams, G.B., Pena, A., Sahakian, B.J., and Pickard, J.D. (2006). Diffusion tensor imaging in chronic head injury survivors: correlations with learning and memory indices. Neuroimage 29, 117–124.
38. Xu, J. Rasmussen, I., Lagopoulos, J., and Haberg, A. (2007). Diffuse axonal injury in severe traumatic brain injury visualized using high-resolution diffusion tensor imaging. J. Neurotrauma 24, 753–765.
39. Niogi, S.N., and Mukherjee, P. (2010). Diffusion tensor imaging of mild traumatic brain injury. J. Head Trauma Rehabil. 25, 241–255.
40. MacDonald, C.L., Dikranian, K., Bayly, P., Holtzman, D., and Brody, D. (2007). Diffusion tensor imaging reliably detects experimental traumatic axonal injury and indicates approximate time of injury. J. Neurosci. 27, 11869–11876.

41. Mayer, A.R., Ling, J., Mannell, M.V., Gasparovic, C., Phillips, J.P., Doezema, D., Reichard, R., and Yeo, R.A. (2010). A prospective diffusion tensor imaging study in mild traumatic brain injury. Neurology 74, 643–650.
42. Farbota, K.D., Bendlin, B.B., Alexander, A.L., Rowley, H.A., Dempsey, R.J., and Johnson, S.C. (2012). Longitudinal diffusion tensor imaging and neuropsychological correlates in traumatic brain injury patients. Front. Hum. Neurosci. 6, 160.
43. Magnoni, S, MacDonald, C.L., Esparza, T.J., Conte, V., Sorrell, J., Macri, M., Bertani, G., Biffi, R., Costa, A., Sammons, B., Snyder, A.Z., Shimony, J.S., Triulzi, F., Stochetti, N., and Brody, D.L. (2015). Quantitative assessments of traumatic axonal injury in human brain: concordance of microdialysis and advanced MRI. Brain 138, 2263–2277.
44. Sener, S., Van Hecke, W., Feyen, B.F., Van der Steen, G., Pullens P., Van de Hauwe L., Menovsky, T., Parizel, P.M., Jorens, P.G., and Maas A.I. (2016). Diffusion tensor imaging: a possible biomarker in severe traumatic brain injury and aneurysmal subarachnoid hemorrhage? Neurosurgery 79:786–793
45. Adamson, C., Yuan, W., Babcock, L., Leach, J.L., Seal, M.L., Holland, S.K., and Wade, S.L. (2013). Diffusion tensor imaging detects white matter abnormalities and associated cognitive deficits in chronic adolescent TBI. Brain Inj. 27, 454–463.
46. Kinnunen, K.M., Greenwood, R., Powell, J.H., Leech, R., Hawkins, P.C., Bonnelle, V., Patel, M.C., Counsell, S.J., and Sharp, D.J. (2011). White matter damage and cognitive impairment after traumatic brain injury. Brain, 134, 449–463.
47. Hashim, E., Caverzasi, E., Papinutto, N., Lewis, C.E., Jing, R., Charles, O., Zhang, S., Lin, A., Graham, S.J., Schweizer, T.A., Bharatha, A., and Cusimano, M.D. (2017). Investigating microstructural abnormalities and neurocognition in subacute and chronic traumatic brain injury patients with normal-appearing white matter: a preliminary diffusion tensor imaging study. Front. Neurol. 8, 97.
48. Spitz, G., Alway, Y., Gould, K.R., and Ponsford, J.L. (2016). Disrupted white matter microstructure and mood disorders after traumatic brain injury. J. Neurotrauma 33, 1–9.
49. Chiou, K.S., Genova, H.M., and Chiaravalloti, N.D. (2015). Structural white matter differences underlying heterogeneous learning abilities after TBI. Brain Imaging Behav. 10, 1274–1279.
50. Strauss, S., Hulkower, M., Gulko, E., Zampolin, R.L., Gutman, D., Chitkara, M., Zughaft, M., and Lipton, M.L. (2105). Current clinical applications and future potential of diffusion tensor imaging in traumatic brain injury. Top. Magn. Reson. Imaging 24, 353–362.
51. Nakayama, N., Okumura, A., Shinoda, J., Yasokawa, Y.-T., Miwa, K., Yoshimura, S.-I., and Iwama, T. (2006). Evidence for white matter disruption in traumatic brain injury without macroscopic lesions. J. Neurol. Neurosurg. Psychiatry 77, 850–855.
52. Moen, K.G., Vik, A., Olsen, A., Skandsen, T., Håberg, A.K., Evensen, K.A., and Eikenes, L. (2016). Traumatic axonal injury: relationships between lesions in the early phase and diffusion tensor imaging parameters in the chronic phase of traumatic brain injury. J. Neurosci. Res. 94, 623–635.

Address correspondence to:
Kristine H. O'Phelan, MD
Department of Neurology
Miller School of Medicine
University of Miami
1120 NW 14th Street
Don Soffer Clinical Research Building 1356
Miami, FL 33136

E-mail: kophelan@med.miami.edu